




Mediator-29 limits *Caenorhabditis elegans* fecundity

Qi Fan,^{1,†} Christopher Tran ^{1,†} Wei Cao ^{1,*} Roger Pocock ^{1,*}

¹Development and Stem Cells Program, Monash Biomedicine Discovery Institute and Department of Anatomy and Developmental Biology, Monash University, Melbourne, Victoria 3800, Australia

*Corresponding authors: Wei Cao, Development and Stem Cells Program, Monash Biomedicine Discovery Institute and Department of Anatomy and Developmental Biology, Monash University, Melbourne, Victoria 3800, Australia. Email: wei.cao@monash.edu; Roger Pocock, Development and Stem Cells Program, Monash Biomedicine Discovery Institute and Department of Anatomy and Developmental Biology, Monash University, Melbourne, Victoria 3800, Australia. Email: roger.pocock@monash.edu

[†]These authors contributed equally to this work.

Mediator is an evolutionarily conserved multiprotein complex that acts as a critical coregulator of RNA polymerase II-mediated transcription. While core Mediator components are broadly required for transcription, others govern specific regulatory modules and signaling pathways. Here, we investigated the function of *MDT-29/MED29* in the *Caenorhabditis elegans* germ line. We found that endogenously tagged *MDT-29* is ubiquitously expressed and concentrated in discrete foci within germ cell nuclei. Functionally, depleting *MDT-29* in the germ line during larval development boosted fecundity. We determined that the increase in progeny production was likely caused by a combination of an expanded germline stem cell pool and decreased germ cell apoptosis. Thus, *MDT-29* may act to optimize specific gene expression programs to control distinct germ cell behaviors, providing flexibility to progeny production in certain environments.

Keywords: *Caenorhabditis elegans*; germ line; proliferation; apoptosis; Mediator complex; RNA interference; auxin-inducible degradation; WormBase

Introduction

Faithful gamete production requires coordinated regulation of germ cell development and behavior. To this end, specific gene regulatory networks control germ cell proliferation (self-renewal), differentiation, survival, and sex determination. These regulatory mechanisms provide robustness to germ cell trajectories but also flexibility under certain environmental and physiological states. Thus, manipulation of specific gene regulatory networks and developmental decisions can affect fecundity.

Mediator is a multisubunit complex with numerous roles in controlling transcription, including bridging interactions between RNA polymerase II and transcription factors (TFs) (Allen and Taatjes 2015). Mediator contains ~30 protein subunits that are grouped into discrete segments: head, middle, tail, and kinase modules (Fig. 1a). In general, the head and middle modules coordinate assembly of the transcriptional preinitiation complex and general recruitment to promoters, whereas the tail and kinase modules facilitate interactions with specific TFs and enhancer elements to regulate specialized developmental programs (Allen and Taatjes 2015). As a result, selectively removing or including tail and kinase module components may give gene regulatory networks flexibility in controlling certain cellular events. Such functional specificity is exemplified by *Caenorhabditis elegans* tail module subunits *MDT-15*, *MDT-23*, and *MDT-24* that control lipid metabolism, stress regulation, muscle development, and responses to pathogen infection (Nicholas and Hodgkin 2004; Taubert et al. 2006; Meissner et al. 2009; Goh et al. 2014; Grants et al. 2015).

Here, we determined the expression and function of *MDT-29* in the *C. elegans* germ line, a previously uncharacterized Mediator tail module component. We found that endogenously tagged *MDT-29* is likely expressed in all cell nuclei. Furthermore, *MDT-29* protein is concentrated in distinct foci, which resemble phase-separated condensates previously discovered to house Mediator components in mammalian cells (Cho et al. 2018; Sabari et al. 2018). We discovered that germline-specific *MDT-29* depletion via RNA-mediated interference (RNAi) knockdown or auxin-inducible degradation (AID) increased cell number within the germline progenitor zone (PZ), which is likely driven independently of the *GLP-1*/Notch signaling pathway. Further analysis suggested that increased cell number in the PZ caused by *MDT-29* depletion is the result of an enlarged germline stem cell pool. In addition, we discovered that *MDT-29* limits physiological apoptosis in oogenic germ cells. Together, these proliferative and cell death phenotypes likely combine to cause the elevated brood size observed in *MDT-29*-depleted hermaphrodites. Thus, *MDT-29* may coordinate specific gene expression programs to govern germ cell proliferation and death to optimize brood size under certain environmental and/or physiological conditions.

Materials and methods

Strains

C. elegans strains were maintained on nematode growth medium (NGM) plates seeded with OP50 *Escherichia coli* bacteria at 20°C, unless otherwise stated. Animals were continuously fed for at least 3

Received on 13 February 2025; accepted on 16 March 2025

© The Author(s) 2025. Published by Oxford University Press on behalf of The Genetics Society of America.

This is an Open Access article distributed under the terms of the Creative Commons Attribution-NonCommercial-NoDerivs licence (<https://creativecommons.org/licenses/by-nc-nd/4.0/>), which permits non-commercial reproduction and distribution of the work, in any medium, provided the original work is not altered or transformed in any way, and that the work is properly cited. For commercial re-use, please contact reprints@oup.com for reprints and translation rights for reprints. All other permissions can be obtained through our RightsLink service via the Permissions link on the article page on our site—for further information please contact journals.permissions@oup.com.

generations prior to analysis. All strains used in this study are listed in [Supplementary Table 1](#).

Endogenous tagging with CRISPR–Cas9

The *degron::GFP::mdt-29* allele was generated using CRISPR–Cas9 genome editing ([Dokshin et al. 2018](#)). The crRNA targeting *mdt-29* was designed and ordered using the online tool provided by <https://sg.idtdna.com> ([Supplementary Table 2](#)). Ultramer primers were used to produce asymmetric–hybrid donor repair templates ([Supplementary Table 2](#)). Next, the injection mixture was introduced into wild-type animals, which contained 2 µg universal tracrRNA, 1.1 µg crRNA, 5 µg Cas9 protein, 4 µg repair template, and *myo-2::mCherry* plasmid (4 ng/µL). F1 progeny of injected wild-type animals were individually isolated, and their progeny were screened for *degron::GFP* insertion using PCR. The insertion was verified by Sanger sequencing.

RNAi experiments

mdt-29 RNAi was performed by the standard feeding protocol ([Fraser et al. 2000](#)). The *mdt-29* RNAi plasmid was obtained from the Vidal RNAi library ([Rual et al. 2004](#)). The *mdt-29* and L4440 (empty vector control) plasmids were transformed into the HT115 *E. coli* strain, and grown in Luria broth media with 100 µg/µl ampicillin at 37°C for 16 h. RNAi bacteria were seeded on RNAi plates (NGM plates + 3 mM IPTG). Selected animals were maintained on RNAi plates for various periods depending on the experiment (described in figure legends).

AID experiments

AID experiments were performed by transferring worms to ethanol (control) or auxin plates ([Zhang et al. 2015](#)). The 400 mM auxin (indole-3 acetic acid, Alfa Aesar, ALFA10556) stock solution was dissolved in ethanol. Auxin plates (1 mM) were prepared by diluting auxin stock solution into NGM agar before pouring plates.

Brood size analysis

Brood size was quantified by counting progeny produced by each worm in the first 4 days of adulthood. L4 worms were picked onto individual NGM plates, allowing egg laying for 24 h. Next, mothers were moved to new plates every 24 h. The number of hatched larvae was counted. If RNAi knockdown or AID was required, the brood size analysis was conducted on RNAi or auxin plates.

Germline staining

Germ lines were isolated from sedated worms before immunostaining. Dissected germ lines were fixed on poly-L-lysine-coated slides by immersing in ice-cold methanol for 1 min and then 3.7% paraformaldehyde for 30 min. Fixed germ lines were washed twice with PBST (PBS + 0.5% Tween 20) and blocked using 30% normal goat serum. Then, germ lines were incubated in primary antibody at 4°C overnight and washed twice with PBST. Next, germ lines were incubated in secondary antibody and DAPI at 20°C for 2 h, followed by 2 PBST washes. Samples were mounted on slides using Fluoroshield mounting media (Sigma). Stained germ lines were imaged using a confocal microscope Leica SP5 (63× objectives). Primary antibodies used were antiphospho-histone H3 (pH3) (Ser10) (06-570, Merk, 1:500) and monoclonal ANTI-FLAG M2 (F1804, Sigma-Aldrich, 1:500). Secondary antibodies used were goat antirabbit 647 (A21245, Invitrogen, 1:1,000) and goat antimouse 555 (A21422, Invitrogen, 1:1,000).

Germline analysis

Germline analysis was performed as previously described ([Gopal et al. 2017](#)). Z-stack images were acquired using a Leica SP5 confocal microscope (63× objectives) and reconstructed into 3D germline models by using Imaris Suite 9 software. Nuclei of mitotic germ cells (PZ) and pachytene germ cells [pachytene region (PR)] exhibit globular morphology. The transition zone (TZ), which accommodates germ cells at leptotene and zygotene stages, was defined as a continuous region where germ cell rows contain over 60% of crescent shape nuclei. The germline region before the TZ is defined as the PZ. The germline region after the TZ but before the germline loop is defined as the PR. Semi-automatic nuclei counting was performed using the Imaris Suite 9 to count germ cell nuclei in each region, as in our previous study ([Gopal et al. 2017](#)). The nuclei diameter of PZ is set as 2.4 µm, and the nuclei diameter of TZ is set as 2.4 µm in width and 1.8 µm in height. The reliability of this method is confirmed as the readout of PZ nuclei number in control samples is within the previously reported range ([Gopal et al. 2017](#)).

Fluorescence microscopy

Worms were anesthetized in 0.01% tetraisoole and mounted on a 5% agarose pad. Images were taken using an Axio Imager M2 fluorescence microscope and analyzed using Zen software (Zeiss).

Analysis of apoptotic germ cells

Apoptotic germ cells were analyzed using SYTO-12 staining. One-day-old adult worms were washed using M9 media and transferred into a prepared 50 µM SYTO-12 solution (Thermo Scientific) containing OP50 bacteria. After incubating at 25°C for 5 h, worms were transferred to freshly seeded NGM plates for 1 h, allowing the expulsion of stained bacteria from the gut. The number of apoptotic germ cells within the germ line (SYTO-12⁺) was counted using fluorescence microscopy.

Estimation of stem cell pool

The stem cell pool was estimated using the *emb-30* assay as previously described ([Cinquin et al. 2010](#)). The *emb-30(tn377); degron::gfp::mdt-29; sun-1p::TIR1::mRuby* strain was maintained at the permissive temperature of 15°C. *emb-30(tn377); degron::gfp::mdt-29; sun-1p::TIR1::mRuby* worms were synchronized at the L4 stage (Christmas-tree substage) and maintained at 15°C for 36 h to grow into adults. These animals were then switched to the restrictive temperature of 25°C for 12.5 h, at which the metaphase-to-anaphase transition was blocked ([Furuta et al. 2000](#)). Germ lines were then isolated and immunostained using DAPI, anti-pH3 (Ser10) antibody to, respectively, visualize nuclei and M-phase cells using a Leica SP5 confocal microscope. Germline stem cells (pH3⁺ cells in the PZ) were quantified using the Imaris Suite 9 software.

Sperm quantification

Sperm quantification was conducted as previously described ([Dufourcq-Sekatcheff et al. 2021](#)). Worms were dissected and fixed on the poly-L-lysine-coated slides. After DAPI staining, z-stack images of spermatheca were obtained using an AxioImager M2 (Zeiss) fluorescence microscope (40× objective). The number of sperm was manually counted using the FIJI (Fiji Is Just) ImageJ 2.14.0/1.54f software.

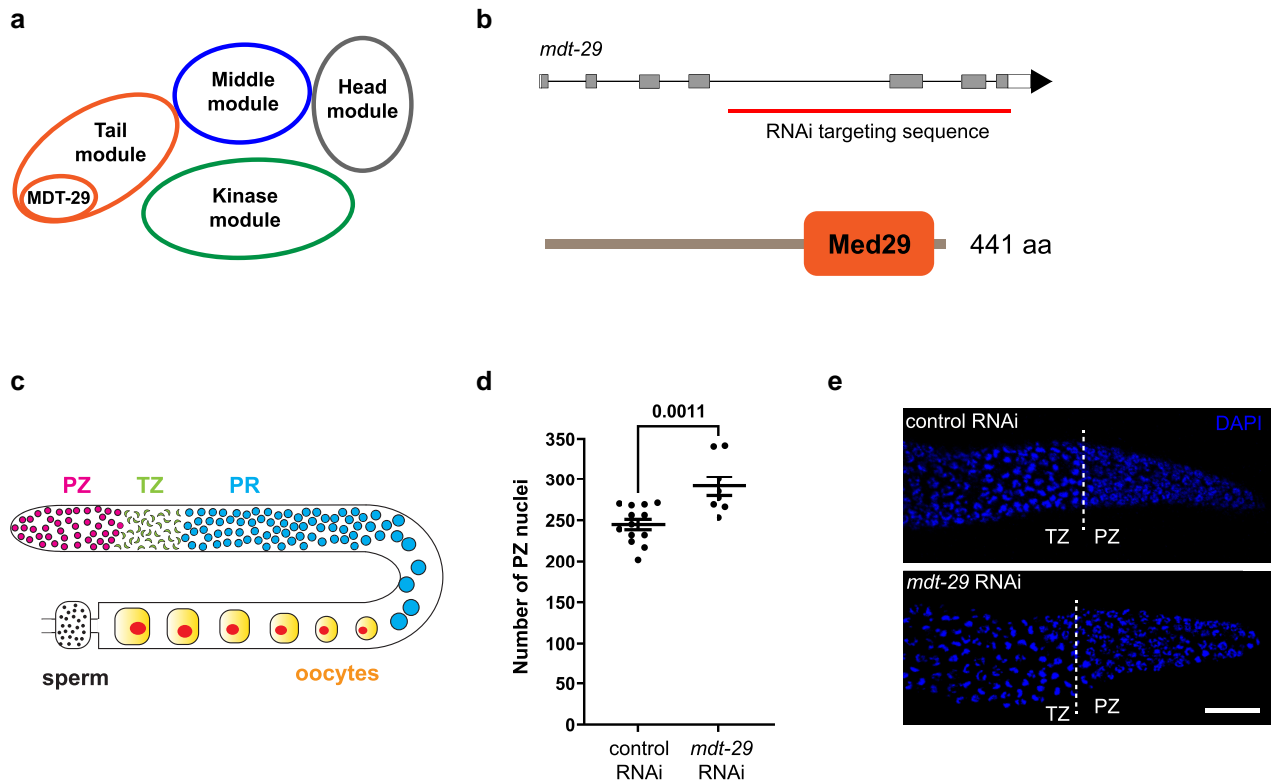


Fig. 1. *mdt-29* RNAi knockdown increases germ cell number in the distal PZ. a) Schematic of the Mediator complex structure showing the head, middle, tail, and kinase modules. The **MDT-29** subunit is shown within the tail module. b) Genomic locus (top—gray boxes = exons; black lines = introns; white boxes = untranslated regions) and protein domain structure (bottom) of **MDT-29**. Med29, Mediator complex subunit 29 domain. Red line = targeting sequence in RNAi experiments. c) Schematic of the *C. elegans* adult hermaphrodite germ line. The germ line contains the PZ (~65% proliferative cells/~35% cells in the meiotic S-phase), the TZ (meiotic prophase cells), and the PR (early meiotic cells), followed by mature gametes (oocytes and sperm). Quantification (d) and immunofluorescence images (e) of germ cell nuclei number in the PZ of *rrf-1(pk1417)* 1-day-old adults following *mdt-29* RNAi knockdown. RNAi treatment commenced in L1 larvae and germ lines of 1-day-old adults were examined. $n = 13, 8$. P-value assessed by unpaired t-test. Data expressed as mean \pm SEM.

Statistical analysis

Statistical analyses were conducted in GraphPad Prism 10 using two-tailed unpaired t-tests or one-way analysis of variance (ANOVA) test. In unpaired t-tests, Welch's correction was applied when significant variance was observed, and the Mann-Whitney test was used when data were not normally distributed. Ordinary two-tailed ANOVA test was performed when data were normally distributed; otherwise, the Kruskal-Wallis test was performed. Brown-Forsythe ANOVA test was performed when significant variance was identified. Specific statistical tests used for each experiment are detailed in the figure legends. Data are expressed as mean \pm SEM. Significant differences was determined with a P-value of < 0.05 .

Results and discussion

MDT-29 is required for *C. elegans* germ cell development

In an ongoing RNAi screen for factors that control germ cell development in *C. elegans*, we identified the uncharacterized gene *mdt-29*. *mdt-29* encodes a protein containing a Mediator complex subunit 29 (MED29) domain that is a predicted tail module component of the Mediator complex (Fig. 1a and b). Mammalian **MDT-29** orthologs (MED29) have been shown to enhance or inhibit cancer cell proliferation depending on the microenvironment (Kuuselo et al. 2011; Yang et al. 2022; Huang et al. 2024).

We assessed **MDT-29** function using *mdt-29* RNAi knockdown in the *rrf-1(pk1417)* strain, which permits germline and limited somatic RNAi activity (Fig. 1c–e) (Zou et al. 2019; Watts et al. 2020). We found that *mdt-29* knockdown from the L1 stage significantly increased nuclei number in the distal PZ, proposing an inhibitory function of **MDT-29** in germ cell proliferation (Fig. 1d and e). Previous structural analysis of the mammalian Mediator complex suggests that **MDT-29**/MED29, as part of the tail module, serves as a docking site for TF binding (Tsai et al. 2014). Thus, **MDT-29** may suppress germ cell proliferation via transcriptional control of specific signaling pathways. To enable tissue-specific exploration of **MDT-29** function, we utilized CRISPR-Cas9 to insert a *degron::green fluorescent protein (gfp)* coding sequence into the 5' end of the *mdt-29* gene in wild-type animals (Fig. 2a) (Dokshin et al. 2018). The degron sequence enables rapid depletion of endogenous **MDT-29** protein using the AID system (Zhang et al. 2015). Compared with wild-type animals, insertion of *degron::GFP* to **MDT-29** did not cause overt germline defects, as shown by germ cell nuclei counts and brood size (Supplementary Fig. 1). Thus, the *degron::gfp::mdt-29* strain is a reliable tool for subsequent **MDT-29** expression and functional analysis.

MDT-29 is ubiquitously expressed in *C. elegans*

We next examined the expression pattern of **MDT-29** in the *degron::gfp::mdt-29* strain. The Mediator complex functions as an important coregulator of polymerase II-mediated transcription and thus is widely expressed in *C. elegans* (Zhang and Emmons 2001;

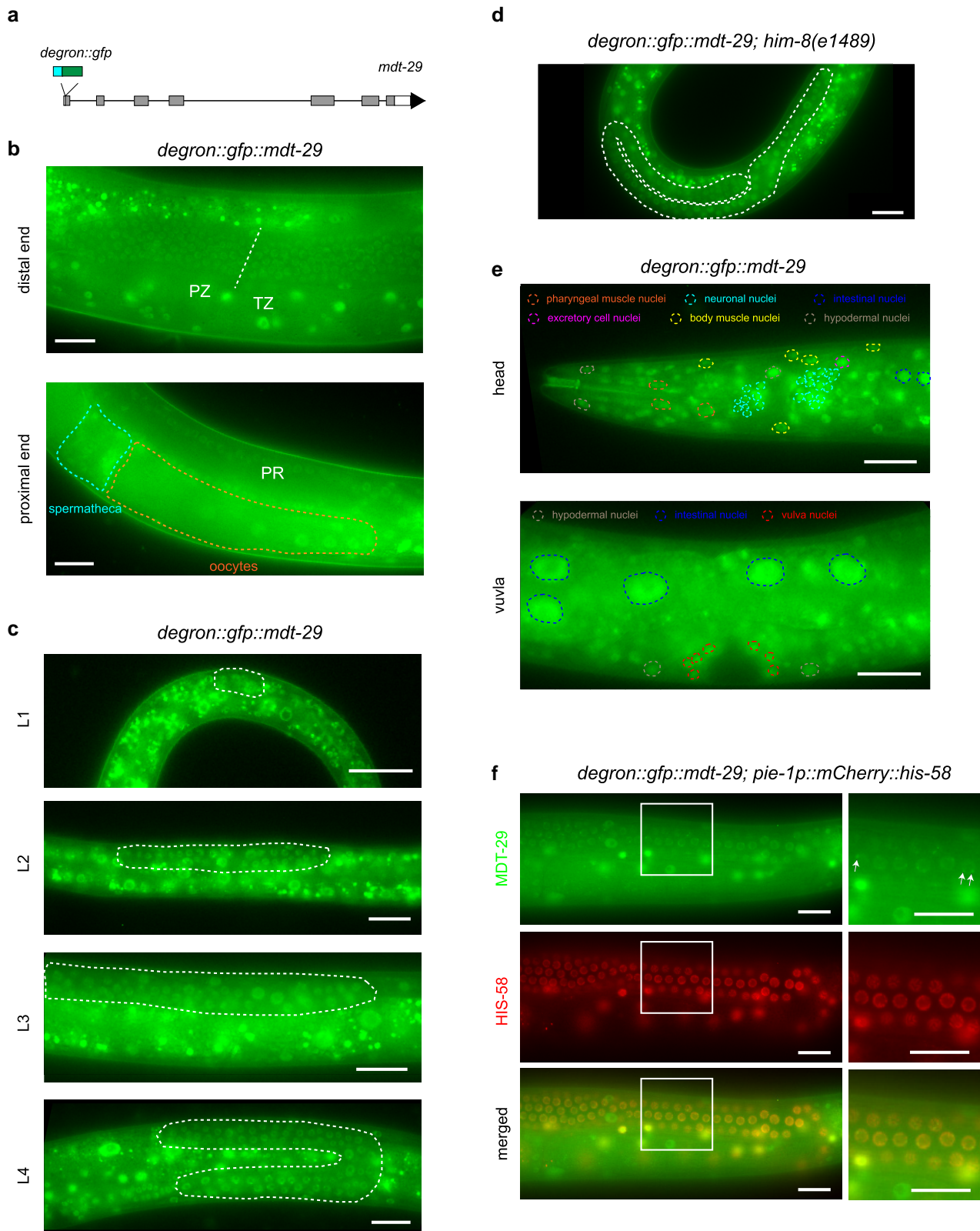


Fig. 2. MDT-29 expression pattern analysis. a) *mdt-29* genomic structure showing insertion of the *degron::gfp* coding sequence at the N terminus. b) Fluorescence micrographs of adult germ lines expressing *degron::GFP::MDT-29*. Expression is detected in the distal end (PZ and TZ—TZ, top image) and proximal end (PR, oocytes and spermatheca, bottom image). White dashed line = border between PZ and TZ. Orange = oocytes. Blue = spermathecum. c) Fluorescence micrographs of larval germ lines expressing *degron::GFP::MDT-29*. Expression detected at the L1, L2, L3, and L4 stages. White dash = germ line. d) Fluorescence micrograph of a male adult germ line expressing *degron::GFP::MDT-29* in *him-8(e1489)* animals. White dash = germ line. e) Fluorescence micrographs of somatic tissues expressing *degron::GFP::MDT-29*. Expression in the head (top) and vulval region (bottom) at the L4 stage. Orange dash = pharyngeal muscle nuclei. Yellow dash = body wall muscle nuclei. Cyan dash = neuronal nuclei. Gray dash = hypodermal nuclei. Blue dash = intestinal nuclei. Magenta dash = excretory cell nucleus. Red dash = vulval nuclei. f) Co-localization of *degron::GFP::MDT-29* and mCherry::HIS-58 in the adult germ line. White arrows indicate *degron::GFP::MDT-29* foci. Green = MDT-29. Red = HIS-58. White box = zoomed region to the right of each image.

Moghal and Sternberg 2003; Taubert et al. 2006; Steimel et al. 2013). Based on previous RNA-seq data, *MDT-29* is expressed in the soma and germ line (Ebbing et al. 2018; Ghaddar et al. 2023). As *mdt-29* RNAi caused overt germline defects (Fig. 1d), we first examined *degron::GFP::MDT-29* expression in the germ line. In adult hermaphrodites, *degron::GFP::MDT-29* expression was detected in all germ cells, including proliferative germ cells (PZ), meiotic cells (TZ and PR), and in gametes (oocytes and sperm) (Fig. 2b). Further, we detected *degron::GFP::MDT-29* expression from early embryogenesis and in germ cells throughout larval development (Fig. 2c; Supplementary Fig. 2). Previous transcriptomic analysis revealed enrichment of *mdt-29* RNA in the male germ line (Ebbing et al. 2018). To examine *MDT-29* expression in males, we crossed the *degron::gfp::mdt-29* animals into the *him-8(e1489)* strain. We detected *degron::GFP::MDT-29* expression throughout the male germ line (Fig. 2d). We also detected *degron::GFP::MDT-29* expression in somatic tissues (pharynx, hypodermis, body wall muscle, intestine, nervous system, vulva, and the excretory system), consistent with RNA-seq data (Fig. 2e) (Ghaddar et al. 2023). Taken together, these observations show that *MDT-29* is likely expressed in all tissues throughout *C. elegans* development in both sexes.

MDT-29 forms condensed foci

While exploring *degron::GFP::MDT-29* expression in the germ line, we observed condensed fluorescent foci within germ cell nuclei, suggesting a specific functional locale for *MDT-29* (Fig. 2f). These *degron::GFP::MDT-29* foci were also observed in somatic tissues and throughout animal development (Fig. 2e). Such foci are reminiscent of phase-separated condensates previously shown to contain Mediator proteins and RNA polymerase II in mammalian cell models (Cho et al. 2018; Sabari et al. 2018). As mammalian mediator condensates associate with chromatin (Cho et al. 2018; Sabari et al. 2018), we assessed this in *C. elegans*. We found that the chromatin reporter mCherry::HIS-58 and *degron::GFP::MDT-29* foci overlap (Fig. 2f). These data imply that, as in mammals, the *C. elegans* Mediator complex localizes and concentrates at discrete nuclear locations.

MDT-29 depletion increases proliferative germ cell number

Our initial RNAi analysis showed that *mdt-29* RNAi knockdown increased germ cell number in the PZ (Fig. 1d). However, RNAi-induced mRNA degradation rarely results in complete gene knockdown and the *rnf-1* mutant strain we used is not absolutely specific for germline RNAi (Watts et al. 2020). We thus turned to the tissue-specific AID system to confirm *MDT-29* germline-specific function. To validate the efficacy of the *degron::gfp::mdt-29* allele for tissue-specific functional analysis, we introduced a transgene (*sun-1p::TIR1::mRuby*) to express the transport inhibitor response 1 (TIR1) F-box protein (required for AID) in the germ line (Zhang et al. 2015). This new strain (*degron::gfp::mdt-29; sun-1p::TIR1::mRuby*) exhibits wild-type germline development in the absence of auxin (Supplementary Fig. 1). We found that within 1 h of auxin exposure *degron::GFP::MDT-29* was efficiently depleted in the adult germ line (Fig. 3a). Therefore, *degron::GFP::MDT-29* can be rapidly depleted using the AID system.

Next, we exposed *degron::gfp::mdt-29; sun-1p::TIR1::mRuby* animals to auxin continuously from the L1 larval stage (called *MDT-29* L1 AID from here) and analyzed the germ lines of 1-day-old adults (Fig. 3b–d). We found that *MDT-29* L1 AID caused an increase in the PZ size, consistent with our findings of *mdt-29* RNAi (Figs. 1d and 3c and d). However, we did not detect a change in cell number within the TZ when cells are entering early meiotic

prophase (Fig. 3c and d). The increase in PZ cell number suggested that *MDT-29* controls germ cell proliferation.

To evaluate the proliferative state of germ cells following *MDT-29* L1 AID, we used an antibody against pH3 to mark dividing germ cells in M-phase (Fig. 3d). The mitotic index (MI) was assessed by calculating the percentage of PZ cells that are at M-phase to signify the mitotic cell cycling activity (Crittenden et al. 2023). We found no significant difference in the MI following *MDT-29* L1 AID, suggesting that *MDT-29* does not regulate mitotic cell cycling (Fig. 3c and d). Together, our RNAi and AID depletion approaches (Figs. 1d and 3c) reveal that *MDT-29* controls PZ germ cell number in *C. elegans*.

MDT-29 regulates the distal germline stem cell pool

The germline PZ accommodates ~65% proliferative cells and ~35% cells in meiotic S-phase (Fox et al. 2011). Germ cell proliferation requires the maintenance of the germline stem cell pool at the distal end. Germline stem cell renewal is stimulated by the interaction of the *GLP-1* Notch receptor expressed on their surface and Notch ligands (*LAG-2/APX-1*) expressed on somatic distal tip cells (Austin and Kimble 1987; Henderson et al. 1994; Gao and Kimble 1995). *GLP-1*/Notch signaling promotes germline stem cell proliferation through 2 redundant transcriptional regulators, *SYGL-1* and *LST-1* (Kershner et al. 2014; Lee et al. 2016; Shin et al. 2017).

The germline stem cell pool can be estimated using the *emb-30* assay (Cinquin et al. 2010). In the *emb-30(tn377)* temperature-sensitive mutant, the metaphase-to-anaphase transition is blocked at the restrictive temperature (25°C). Therefore, arrested mitotic germ cells, visualized by pH3 immunostaining, represent the entire germline stem cell pool. To assess the role of *MDT-29* in germline stem cell pool maintenance, we introduced the *emb-30(tn377)* mutant into the *MDT-29* AID strain. *emb-30(tn377); MDT-29* AID L1 animals were exposed to auxin at 15°C for 106 h and then shifted to the restrictive temperature of 25°C for 12.5 h as adults (Fig. 3e). We found that *MDT-29* L1 AID increased the germline stem cell pool size by ~20% (Fig. 3f and g). Importantly, auxin exposure alone did not affect the maintenance of germline stem cell pool in *emb-30(tn377)* animals (Supplementary Fig. 3). These results suggest that the increased PZ size induced by *MDT-29* L1 AID likely occurs through regulation of the germline stem cell pool.

MDT-29 was previously identified as a putative transcriptional co-activator in the *LIN-12*/Notch signaling pathway to facilitate the formation of a transient nuclear complex (Chen et al. 2004). Therefore, we hypothesized that *MDT-29* also acts as a co-activator in the related *GLP-1*/Notch signaling pathway. To investigate this hypothesis, we analyzed the expression of the *GLP-1*/Notch targets *SYGL-1* and *LST-1* in the germ line. To this end, we individually crossed endogenously tagged *SYGL-1* (3xflag::sygl-1) and *LST-1* (3xflag::lst-1) animals with the *MDT-29* AID strain (Shin et al. 2017) and counted the number of germ cells in the *SYGL-1*⁺/*LST-1*⁺ expression domains (Shin et al. 2017; Chen et al. 2020). However, we found that *MDT-29* L1 AID does not affect the number of *SYGL-1*⁺ or *LST-1*⁺ germ cells (Fig. 3h–k). These data suggest that the increase in the germline stem cell pool size following *MDT-29* L1 AID does not result from altered *GLP-1*/Notch signaling.

MDT-29 regulates fecundity

In *C. elegans* hermaphrodites, as germ cells move proximally, mitotic germ cells transit through meiosis and develop into sperm

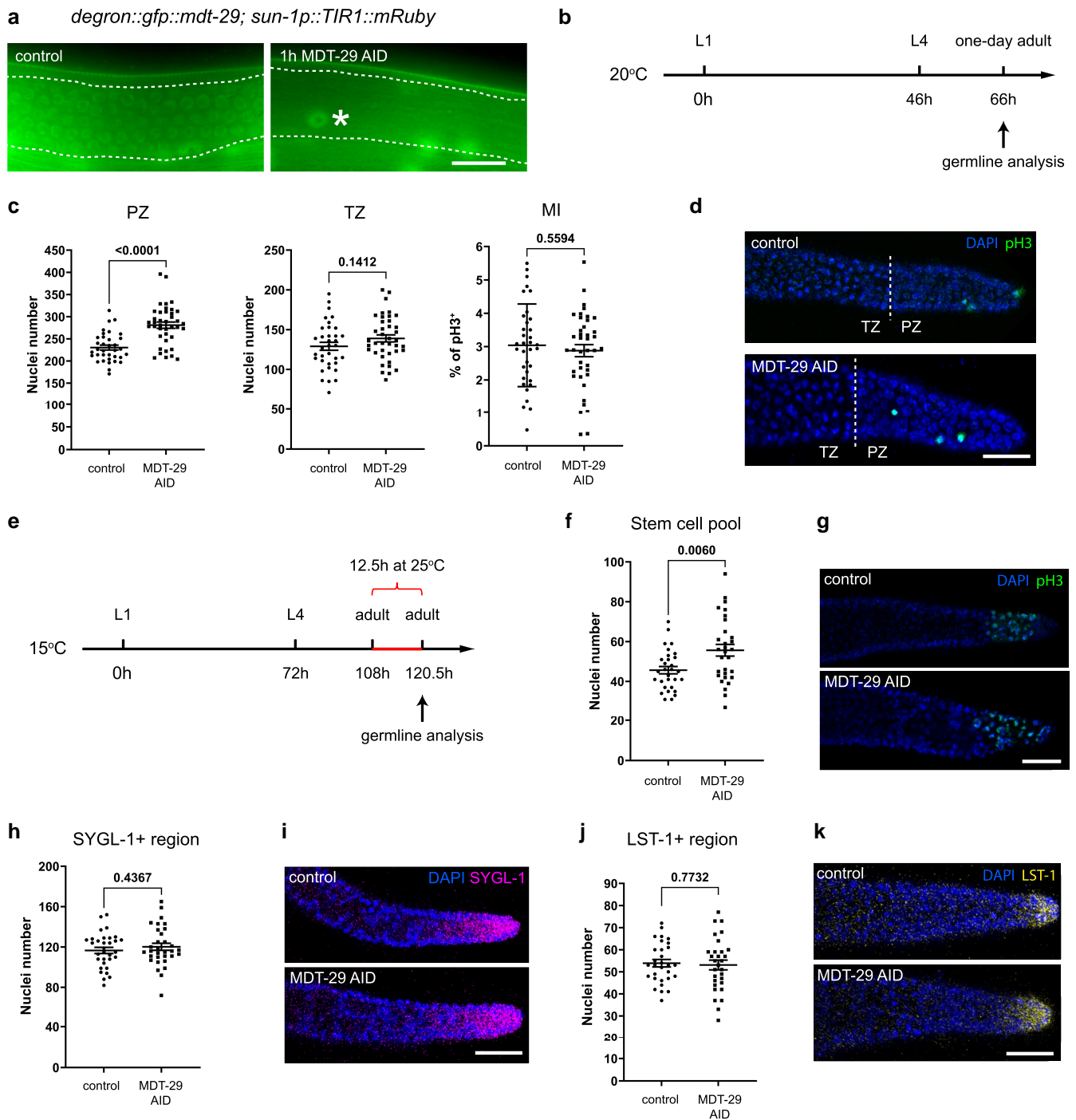


Fig. 3. MDT-29 regulation of distal germ cell proliferation. **a)** Fluorescence micrographs of *degron::gfp::mdt-29; sun-1p::TIR1::mRuby* animals treated with ethanol (control) or auxin for 1 h. *sun-1p::TIR1::mRuby* = germline-specific AID strain. White dashed line = germ line region. The large GFP-positive nucleus (white asterisk) within the dashed line in the 1-h MDT-29 AID image is an intestinal nucleus. **b)** Timeline of germline analysis following L1 auxin treatment. Freshly hatched L1 animals were transferred to ethanol or auxin plates and incubated at 20°C for 66 h, and germlines were dissected in 1-day-old adults. Animals were confirmed as L4 larvae at 46 h. Quantification (**c**) and immunofluorescence images (**d**) of germ cell number of PZ and TZ, and MI of *degron::gfp::mdt-29; sun-1p::TIR1::mRuby* 1-day-old adults treated with ethanol (control) or auxin for 1 h. Germ lines were stained with DAPI to visualize DNA (blue) and anti-pH3 to visualize M-phase chromosomes (green). White dashed line = border between PZ and TZ. $n = 35, 40$. **e)** Timeline of stem cell pool evaluation following MDT-29 AID from the L1 stage. Freshly hatched L1 animals were transferred to ethanol or auxin plates and incubated at 15°C for 108 h, and these 1-day-old adults were heat-shocked at 25°C for 12.5 h; then, their germ lines were dissected and stained at 120.5 h. Animals were confirmed as L4 larvae at 72 h. Quantification (**f**) and immunofluorescence images (**g**) of germline stem cells of *emb-30(tn377); degron::gfp::mdt-29; sun-1p::TIR1::mRuby* 1-day-old adults. Germ lines were stained with DAPI to visualize DNA (blue) and anti-pH3 to visualize M-phase chromosomes (green). $n = 30$. Quantification (**h**) and immunofluorescence images (**i**) of SYGL-1⁺ germ cells of *3xflag::sygl-1; degron::gfp::mdt-29; sun-1p::TIR1::mRuby* 1-day-old adults. Germ lines were stained with DAPI to visualize DNA (blue) and anti-FLAG antibodies to visualize SYGL-1⁺ germ cells (pink). $n = 32$. Quantification (**j**) and immunofluorescence images (**k**) of LST-1⁺ cells of *3xflag::lst-1; degron::gfp::mdt-29; sun-1p::TIR1::mRuby* 1-day-old adults. Germ lines were stained with DAPI to visualize DNA (blue) and anti-FLAG antibodies to visualize LST-1⁺ germ cells (yellow). $n = 30$. Ethanol was applied in the control group. MDT-29 AID commenced from the L1 stage. Data expressed as mean \pm SEM. P values assessed by unpaired t-test (**c**, **h**, and **j**) and Welch's t-test (**f**). Scale bars = 20 μ m.

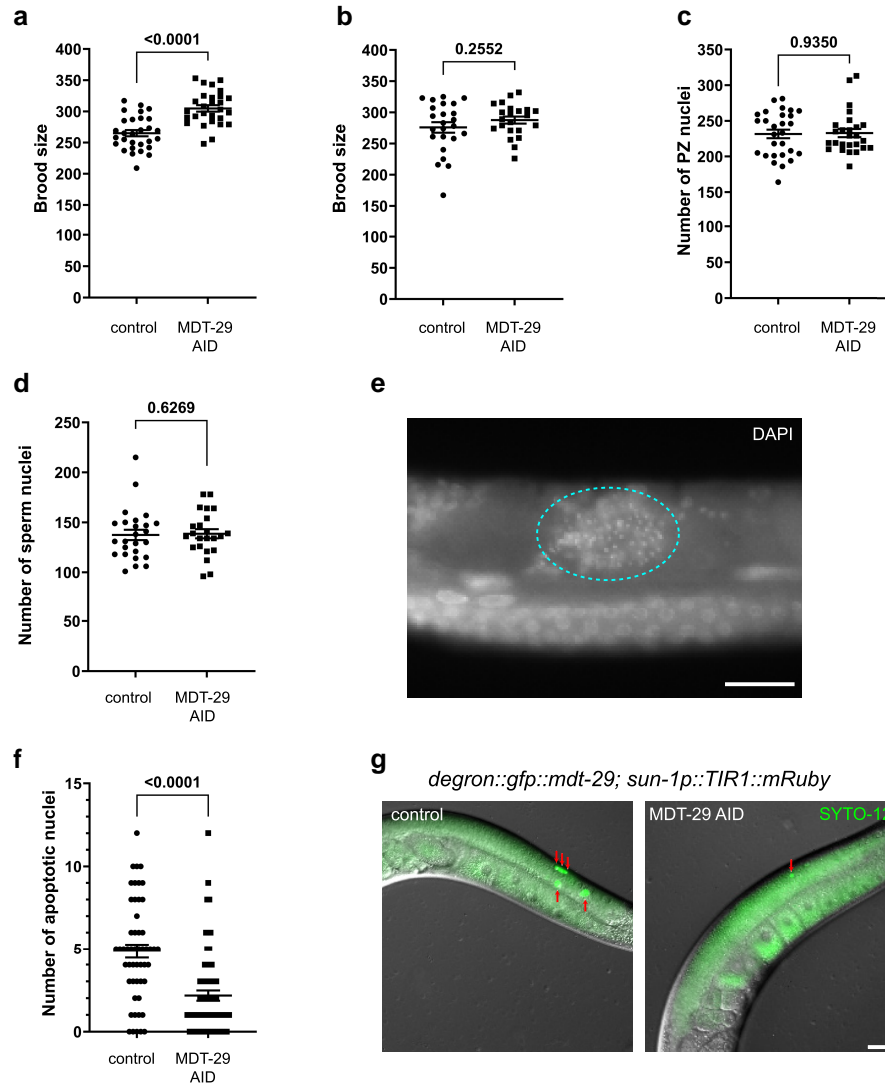


Fig. 4. MDT-29 regulation of progeny production. a) Brood size quantification of *degren::gfp::mdt-29; sun-1p::TIR1::mRuby* hermaphrodites following MDT-29 L1 AID. $n = 29, 28$. b) Brood size quantification of *degren::gfp::mdt-29; sun-1p::TIR1::mRuby* hermaphrodites following L4 AID. $n = 22, 24$. c) Quantification of PZ germ cell number of *degren::gfp::mdt-29; sun-1p::TIR1::mRuby* 1-day-old adults following AID treatment from the L4 stage. $n = 26, 28$. Quantification (d) and immunofluorescence images (e) of sperm of *degren::gfp::mdt-29; sun-1p::TIR1::mRuby* 1-day-old adults. Cyan dash = spermathecum. $n = 25, 23$. Quantification (f) and fluorescence micrographs (g) of apoptotic germ cells. SYTO-12 staining was performed following MDT-29 L1 AID. $n = 52, 65$. Red arrows = apoptotic germ cells. Ethanol was applied in the control group. Data expressed as mean \pm SEM. P values assessed by unpaired t-test (a and b) and Mann-Whitney test (c, d, and f). Scale bar = $20 \mu\text{m}$.

during the L4 larval stage before switching to the oogenesis program in adulthood (Kulkarni et al. 2012). Following meiotic maturation, oocytes are fertilized by sperm and then commence embryogenesis. As MDT-29 is required for proper germ cell proliferation, we examined whether the increase in PZ cell number following MDT-29 AID leads to a difference in progeny output. We found that MDT-29 L1 AID indeed increases the brood size by $\sim 15\%$ (Fig. 4a). We next examined MDT-29 function during gametogenesis, by performing MDT-29 AID from L4, when spermatogenesis initiates. We found that MDT-29 L4 AID did not affect PZ cell number or brood size (Fig. 4b and c). These results suggest that MDT-29 is not essential for late germline development and likely acts earlier during larval development to regulate germ cell proliferation.

Because sperm number is a limiting factor in brood size, we investigated whether MDT-29 AID affects the number of sperm. We quantified sperm number of MDT-29 L1 AID 1-day-old adults

following germline dissection and DAPI staining and found that MDT-29 L1 AID did not affect sperm number (Fig. 4d and e). Potentially, however, an increase in fertilization rate may mask any small change in sperm number that would be sufficient to cause the increase in brood size. During meiotic development, more than half of oogenic germ cells undergo physiological apoptosis around the germline loop to supply cytoplasmic components for maturing oocytes (Gumienny et al. 1999; Hubbard and Schedl 2019). Thus, the number of progeny generated can also be affected by apoptosis. We thus labeled apoptotic germ cells using SYTO-12 following MDT-29 L1 AID, as previously described (Fig. 4f and g) (Gumienny et al. 1999). We found that MDT-29 L1 AID reduced the number of apoptotic cells in the PR. Therefore, reduced germ cell apoptosis may contribute to the increase in brood size observed when MDT-29 is depleted in the germ line.

Taken together, our study reveals that MDT-29, a tail module Mediator complex component, limits fecundity in *C. elegans*. Our

analysis of germ cell behavior suggests that **MDT-29** controls progeny production by modulating the germline stem cell pool size and germ cell apoptosis. Thus, **MDT-29** likely controls discrete gene regulatory networks to control germ cell behavior by coordinating with context-specific TFs.

Data availability

All data are available in the main text, [Supplementary materials](#), and source data. No accession codes, unique identifiers, or weblinks are in our study, and there are no restrictions on data availability. Materials are available upon request from Roger Pocock.

[Supplemental material](#) available at GENETICS online.

Acknowledgments

The authors thank members of the Pocock for advice and comments on the manuscript. Imaging was performed at Monash Microimaging. Some strains were provided by the Caenorhabditis Genetics Center (University of Minnesota), which is funded by the NIH Office of Research Infrastructure Programs (P40 OD010440).

Funding

This work was supported by the following grants: Australian Research Council DP200103293 (R.P.) and National Health and Medical Research Council GNT1105374 (R.P.), GNT1137645 (R.P.), and GNT2018825 (R.P., W.C., and Q.F.).

Conflicts of interest

The authors declare that they have no competing interests.

Author contributions

W.C. and R.P. were involved in conceptualization and supervision. Q.F., W.C., and R.P. were involved in funding acquisition. Q.F. was involved in writing—original draft. All authors were involved in methodology, investigation, visualization, project administration, and writing—review and editing.

Literature cited

- Allen BL, Taatjes DJ. 2015. The Mediator complex: a central integrator of transcription. *Nat Rev Mol Cell Biol.* 16(3):155–166. doi:[10.1038/nrm3951](#).
- Austin J, Kimble J. 1987. *glp-1* is required in the germ line for regulation of the decision between mitosis and meiosis in *C. elegans*. *Cell.* 51(4):589–599. doi:[10.1016/0092-8674\(87\)90128-0](#).
- Chen J, Li X, Greenwald I. 2004. *sel-7*, a positive regulator of *lin-12* activity, encodes a novel nuclear protein in *Caenorhabditis elegans*. *Genetics.* 166(1):151–160. doi:[10.1534/genetics.166.1.151](#).
- Chen J, Mohammad A, Pazdernik N, Huang H, Bowman B, Tycksen E, Schedl T. 2020. GLP-1 Notch-LAG-1 CSL control of the germline stem cell fate is mediated by transcriptional targets *lst-1* and *sygl-1*. *PLoS Genet.* 16(3):e1008650. doi:[10.1371/journal.pgen.1008650](#).
- Cho WK, Spille JH, Hecht M, Lee C, Li C, Grube V, Cisse II. 2018. Mediator and RNA polymerase II clusters associate in transcription-dependent condensates. *Science.* 361(6400):412–415. doi:[10.1126/science.aar4199](#).
- Cinquin O, Crittenden SL, Morgan DE, Kimble J. 2010. Progression from a stem cell-like state to early differentiation in the *C. elegans* germ line. *Proc Natl Acad Sci U S A.* 107(5):2048–2053. doi:[10.1073/pnas.0912704107](#).
- Crittenden SL, Seidel HS, Kimble J. 2023. Analysis of the *C. elegans* germline stem cell pool. *Methods Mol Biol.* 2677:1–36. doi:[10.1007/978-1-0716-3259-8_1](#).
- Dokshin GA, Ghanta KS, Piscopo KM, Mello CC. 2018. Robust genome editing with short single-stranded and long, partially single-stranded DNA donors in *Caenorhabditis elegans*. *Genetics.* 210(3):781–787. doi:[10.1534/genetics.118.301532](#).
- Dufourcq-Sekatcheff E, Cuine S, Li-Beisson Y, Quevarec L, Richaud M, Galas S, Frelon S. 2021. Deciphering differential life stage radioinduced reproductive decline in *Caenorhabditis elegans* through lipid analysis. *Int J Mol Sci.* 22(19):10277. doi:[10.3390/ijms221910277](#).
- Ebbing A, Vertesy A, Betist MC, Spanjaard B, Junker JP, Berezhikov E, van Oudenaarden A, Korswagen HC. 2018. Spatial transcriptomics of *C. elegans* males and hermaphrodites identifies sex-specific differences in gene expression patterns. *Dev Cell.* 47(6):801–813 e806. doi:[10.1016/j.devcel.2018.10.016](#).
- Fox PM, Vought VE, Hanazawa M, Lee MH, Maine EM, Schedl T. 2011. Cyclin E and CDK-2 regulate proliferative cell fate and cell cycle progression in the *C. elegans* germline. *Development.* 138(11):2223–2234. doi:[10.1242/dev.059535](#).
- Fraser AG, Kamath RS, Zipperlen P, Martinez-Campos M, Sohrmann M, Ahringer J. 2000. Functional genomic analysis of *C. elegans* chromosome I by systematic RNA interference. *Nature.* 408(6810):325–330. doi:[10.1038/35042517](#).
- Furuta T, Tuck S, Kirchner J, Koch B, Auty R, Kitagawa R, Rose AM, Greenstein D. 2000. EMB-30: an APC4 homologue required for metaphase-to-anaphase transitions during meiosis and mitosis in *Caenorhabditis elegans*. *Mol Biol Cell.* 11(4):1401–1419. doi:[10.1091/mbc.11.4.1401](#).
- Gao D, Kimble J. 1995. APX-1 can substitute for its homolog LAG-2 to direct cell interactions throughout *Caenorhabditis elegans* development. *Proc Natl Acad Sci U S A.* 92(21):9839–9842. doi:[10.1073/pnas.92.21.9839](#).
- Ghaddar A, Armingol E, Huynh C, Gevitzman L, Lewis NE, Waterston R, O'Rourke EJ. 2023. Whole-body gene expression atlas of an adult metazoan. *Sci Adv.* 9(25):eadg0506. doi:[10.1126/sciadv.adg0506](#).
- Goh GY, Martelli KL, Parhar KS, Kwong AW, Wong MA, Mah A, Hou NS, Taubert S. 2014. The conserved Mediator subunit MDT-15 is required for oxidative stress responses in *Caenorhabditis elegans*. *Aging Cell.* 13(1):70–79. doi:[10.1111/accel.12154](#).
- Gopal S, Boag P, Pocock R. 2017. Automated three-dimensional reconstruction of the *Caenorhabditis elegans* germline. *Dev Biol.* 432(2):222–228. doi:[10.1016/j.ydbio.2017.10.004](#).
- Grants JM, Goh GY, Taubert S. 2015. The Mediator complex of *Caenorhabditis elegans*: insights into the developmental and physiological roles of a conserved transcriptional coregulator. *Nucleic Acids Res.* 43(4):2442–2453. doi:[10.1093/nar/gkv037](#).
- Gumienny TL, Lambie E, Hartwig E, Horvitz HR, Hengartner MO. 1999. Genetic control of programmed cell death in the *Caenorhabditis elegans* hermaphrodite germline. *Development.* 126(5):1011–1022. doi:[10.1242/dev.126.5.1011](#).
- Henderson ST, Gao D, Lambie EJ, Kimble J. 1994. *lag-2* may encode a signaling ligand for the GLP-1 and LIN-12 receptors of *C. elegans*. *Development.* 120(10):2913–2924. doi:[10.1242/dev.120.10.2913](#).
- Huang S, Zhang J, Qiao Y, Pathak JL, Zou R, Piao Z, Xie S, Liang J, Ouyang K. 2024. CHRDL1 inhibits OSCC metastasis via MAPK signaling-mediated inhibition of MED29. *Mol Med.* 30(1):187. doi:[10.1186/s10020-024-00956-y](#).

- Hubbard EJA, Schedl T. 2019. Biology of the *Caenorhabditis elegans* germline stem cell system. *Genetics*. 213(4):1145–1188. doi:[10.1534/genetics.119.300238](https://doi.org/10.1534/genetics.119.300238).
- Kershner AM, Shin H, Hansen TJ, Kimble J. 2014. Discovery of two GLP-1/Notch target genes that account for the role of GLP-1/Notch signaling in stem cell maintenance. *Proc Natl Acad Sci U S A*. 111(10):3739–3744. doi:[10.1073/pnas.1401861111](https://doi.org/10.1073/pnas.1401861111).
- Kulkarni M, Shakes DC, Guevel K, Smith HE. 2012. SPE-44 implements sperm cell fate. *PLoS Genet*. 8(4):e1002678. doi:[10.1371/journal.pgen.1002678](https://doi.org/10.1371/journal.pgen.1002678).
- Kuuselo R, Savinainen K, Sandstrom S, Autio R, Kallioniemi A. 2011. MED29, a component of the mediator complex, possesses both oncogenic and tumor suppressive characteristics in pancreatic cancer. *Int J Cancer*. 129(11):2553–2565. doi:[10.1002/ijc.25924](https://doi.org/10.1002/ijc.25924).
- Lee C, Sorensen EB, Lynch TR, Kimble J. 2016. *C. elegans* GLP-1/Notch activates transcription in a probability gradient across the germline stem cell pool. *Elife*. 5:e18370. doi:[10.7554/eLife.18370](https://doi.org/10.7554/eLife.18370).
- Meissner B, Warner A, Wong K, Dube N, Lorch A, McKay SJ, Khattra J, Rogalski T, Somasiri A, Chaudhry I, et al. 2009. An integrated strategy to study muscle development and myofilament structure in *Caenorhabditis elegans*. *PLoS Genet*. 5(6):e1000537. doi:[10.1371/journal.pgen.1000537](https://doi.org/10.1371/journal.pgen.1000537).
- Moghal N, Sternberg PW. 2003. A component of the transcriptional mediator complex inhibits RAS-dependent vulval fate specification in *C. elegans*. *Development*. 130(1):57–69. doi:[10.1242/dev.00189](https://doi.org/10.1242/dev.00189).
- Nicholas HR, Hodgkin J. 2004. The ERK MAP kinase cascade mediates tail swelling and a protective response to rectal infection in *C. elegans*. *Curr Biol*. 14(14):1256–1261. doi:[10.1016/j.cub.2004.07.022](https://doi.org/10.1016/j.cub.2004.07.022).
- Rual JF, Ceron J, Koreth J, Hao T, Nicot AS, Hirozane-Kishikawa T, Vandenhaute J, Orkin SH, Hill DE, van den Heuvel S, et al. 2004. Toward improving *Caenorhabditis elegans* phenome mapping with an ORFeome-based RNAi library. *Genome Res*. 14(10b):2162–2168. doi:[10.1101/gr.2505604](https://doi.org/10.1101/gr.2505604).
- Sabari BR, Dall'Agnese A, Boija A, Klein IA, Coffey EL, Shrinivas K, Abraham BJ, Hannett NM, Zamudio AV, Manteiga JC, et al. 2018. Coactivator condensation at super-enhancers links phase separation and gene control. *Science*. 361(6400):eaar3958. doi:[10.1126/science.aar3958](https://doi.org/10.1126/science.aar3958).
- Shin H, Haupt KA, Kershner AM, Kroll-Conner P, Wickens M, Kimble J. 2017. SYGL-1 and LST-1 link niche signaling to PUF RNA repression for stem cell maintenance in *Caenorhabditis elegans*. *PLoS Genet*. 13(12):e1007121. doi:[10.1371/journal.pgen.1007121](https://doi.org/10.1371/journal.pgen.1007121).
- Steimel A, Suh J, Hussainkhel A, Dehesi S, Grants JM, Zapf R, Moerman DG, Taubert S, Hutter H. 2013. The *C. elegans* CDK8 Mediator module regulates axon guidance decisions in the ventral nerve cord and during dorsal axon navigation. *Dev Biol*. 377(2):385–398. doi:[10.1016/j.ydbio.2013.02.009](https://doi.org/10.1016/j.ydbio.2013.02.009).
- Taubert S, Van Gilst MR, Hansen M, Yamamoto KR. 2006. A Mediator subunit, MDT-15, integrates regulation of fatty acid metabolism by NHR-49-dependent and -independent pathways in *C. elegans*. *Genes Dev*. 20(9):1137–1149. doi:[10.1101/gad.1395406](https://doi.org/10.1101/gad.1395406).
- Tsai KL, Tomomori-Sato C, Sato S, Conaway RC, Conaway JW, Asturias FJ. 2014. Subunit architecture and functional modular rearrangements of the transcriptional mediator complex. *Cell*. 158(2):463. doi:[10.1016/j.cell.2014.06.036](https://doi.org/10.1016/j.cell.2014.06.036).
- Watts JS, Harrison HF, Omi S, Guenther Q, Dalelio J, Pujol N, Watts JL. 2020. New strains for tissue-specific RNAi studies in *Caenorhabditis elegans*. *G3 (Bethesda)*. 10(11):4167–4176. doi:[10.1534/g3.120.401749](https://doi.org/10.1534/g3.120.401749).
- Yang W, Gao K, Qian Y, Huang Y, Xiang Q, Chen C, Chen Q, Wang Y, Fang F, He Q, et al. 2022. A novel tRNA-derived fragment AS-tDR-007333 promotes the malignancy of NSCLC via the HSPB1/MED29 and ELK4/MED29 axes. *J Hematol Oncol*. 15(1):53. doi:[10.1186/s13045-022-01270-y](https://doi.org/10.1186/s13045-022-01270-y).
- Zhang H, Emmons SW. 2001. The novel *C. elegans* gene sop-3 modulates Wnt signaling to regulate Hox gene expression. *Development*. 128(5):767–777. doi:[10.1242/dev.128.5.767](https://doi.org/10.1242/dev.128.5.767).
- Zhang LY, Ward JD, Cheng Z, Dernburg AF. 2015. The auxin-inducible degradation (AID) system enables versatile conditional protein depletion in *C. elegans*. *Development*. 142(24):4374–4384. doi:[10.1242/dev.129635](https://doi.org/10.1242/dev.129635).
- Zou L, Wu D, Zang X, Wang Z, Wu Z, Chen D. 2019. Construction of a germline-specific RNAi tool in *C. elegans*. *Sci Rep*. 9(1):2354. doi:[10.1038/s41598-019-38950-8](https://doi.org/10.1038/s41598-019-38950-8).

Editor: B. Conradt